Reduction in Ocean Heat Transport at 26°N since 2008 Cools the Eastern Subpolar Gyre of the North Atlantic Ocean

Harry L. Bryden,[a] William E. Johns,[b] Brian A. King,[c] Gerard McCarthy,[d]
Elaine L. McDonagh,[c,e] Ben I. Moat,[c] and David A. Smeed[c]

[a] *School of Ocean and Earth Science, University of Southampton, Southampton, United Kingdom*
[b] *Rosenstiel School of Marine and Atmospheric Science, University of Miami, Miami, Florida*
[c] *National Oceanography Centre, Southampton, Southampton, United Kingdom*
[d] *Irish Climate Analysis and Research Units, Department of Geography, Maynooth University, Maynooth, Ireland*
[e] *Norwegian Research Centre, Bjerknes Centre for Climate Research, Bergen, Norway*

(Manuscript received 3 May 2019, in final form 15 November 2019)

ABSTRACT

Northward ocean heat transport at 26°N in the Atlantic Ocean has been measured since 2004. The ocean heat transport is large—approximately 1.25 PW, and on interannual time scales it exhibits surprisingly large temporal variability. There has been a long-term reduction in ocean heat transport of 0.17 PW from 1.32 PW before 2009 to 1.15 PW after 2009 (2009–16) on an annual average basis associated with a 2.5-Sv (1 Sv ≡ $10^6 \, \mathrm{m}^3 \, \mathrm{s}^{-1}$) drop in the Atlantic meridional overturning circulation (AMOC). The reduction in the AMOC has cooled and freshened the upper ocean north of 26°N over an area following the offshore edge of the Gulf Stream/North Atlantic Current from the Bahamas to Iceland. Cooling peaks south of Iceland where surface temperatures are as much as 2°C cooler in 2016 than they were in 2008. Heat uptake by the atmosphere appears to have been affected particularly along the path of the North Atlantic Current. For the reduction in ocean heat transport, changes in ocean heat content account for about one-quarter of the long-term reduction in ocean heat transport while reduced heat uptake by the atmosphere appears to account for the remainder of the change in ocean heat transport.

1. Introduction

The Rapid Climate Change–Meridional Overturning Circulation and Heatflux Array–Western Boundary Time Series (RAPID–MOCHA–WBTS) project has been measuring the Atlantic meridional overturning circulation (AMOC) and its components at 26°N on a continuous basis since March 2004 using a moored array of instruments deployed across the Atlantic Ocean from Florida to the coast of Africa (Fig. 1; Smeed et al. 2018). Prior to 2004, there were historic estimates of the AMOC based on transatlantic hydrographic sections in 1957, 1981, 1992, 1998, and 2004 that suggested there was a long-term decline in AMOC strength (Bryden et al. 2005). The continuous monitoring since March 2004 has shown strong variability in the AMOC on seasonal and shorter time scales that may have aliased these estimates of long-term decline of the AMOC

(Cunningham et al. 2007; Kanzow et al. 2010). On interannual time scales the continuous observations exhibit an event in 2009–10 in which the AMOC dropped by 30% (5.6 Sv) (1 Sv ≡ $10^6 \, \mathrm{m}^3 \, \mathrm{s}^{-1}$) over a 15-month period and subsequently recovered (McCarthy et al. 2012) and a longer-term 2.5-Sv reduction in the AMOC after 2009 that has persisted through 2016 (Smeed et al. 2018).

For the suggested long-term decline in the AMOC from 1957 to 2004, for the 2009–10 event, and for the 2.5-Sv reduction in the AMOC after 2009, the changes in the AMOC are the result of a decrease in the southward flow of Lower North Atlantic Deep Water (LNADW) below 3000-m depth and a compensating increase in the southward recirculation of thermocline waters above 1000-m depth at 26°N (Bryden et al. 2005; McCarthy et al. 2012; Smeed et al. 2018). In the words of McCarthy et al. (2012), for each change there is "less overturning and more recirculation." For all variations, there are only small changes in northward Gulf Stream flow at 26°N. Our interpretation of these changes in the upper water

---

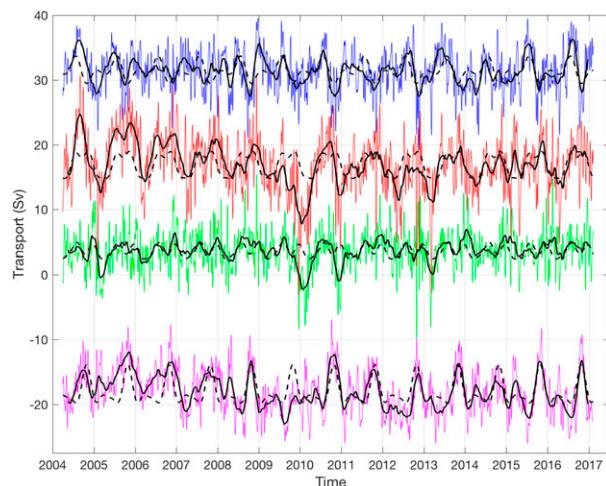*Corresponding author*: Harry L. Bryden, h.bryden@noc.soton.ac.uk

FIG. 1. AMOC time series with components for 2004–17: Gulf Stream transport through Florida Straits (blue), midocean thermocline flow east of the Bahamas (magenta), and wind-driven surface Ekman transport (green)—the sum of these three components is the AMOC (red). Colored lines show 10-day filtered data, black lines are 90-day low-pass-filtered data, and dashed lines show the mean seasonal cycles (Smeed et al. 2018). Annual average values from April to March are given in the supplementary material from Smeed et al. (2018).

circulation is that more of the warm northward-flowing Gulf Stream waters recirculate southward within the subtropical gyre and less-warm waters penetrate northward in the North Atlantic Current into the subpolar gyre. These changes suggest a mode of ocean climate variability in which a reduction in southward deep water flow is compensated by an increase in thermocline recirculation in the subtropical gyre with no sizeable changes in Gulf Stream or Ekman layer transports.

2. Heat and freshwater transports

A companion analysis within the RAPID project has been to determine the time variability of the meridional ocean heat transport across 26°N using the RAPID velocity and temperature measurements combined with midocean temperature profiles derived primarily from XBT and now Argo profiles (Johns et al. 2011). The AMOC circulation, where warm upper waters flow northward and are balanced by southward flow of cold deep waters, results in a northward ocean heat transport of about 1.25 PW at 26°N. Short-term variations in the AMOC are correlated with variations in heat transport with the AMOC accounting for 90% of the total heat transport (Johns et al. 2011). The remaining 10% of the northward heat transport is contributed by the horizontal gyre circulation. Johns et al. estimated that a 1-Sv decline in the AMOC results in a reduction in heat

transport of 0.064 PW. Thus, the 2.5-Sv reduction in the AMOC from before 2009 to after 2009 is expected to reduce the northward heat transport at 26°N by about 0.16 PW. In fact, the average northward ocean heat transport from April 2004 to March 2009 was 1.32 PW and the average ocean heat transport from 2009 to 2016 after the 2.5-Sv reduction in the AMOC was 1.15 PW (Fig. 2), indicating a reduction in heat transport of 0.17 PW.

A second companion analysis within the RAPID project has been to determine the time variability in meridional freshwater transport across 26°N using the RAPID velocity and salinity measurements combined with midocean salinity derived from Argo profiles (McDonagh et al. 2015). The AMOC, where the flow of saltier upper waters northward in the Gulf Stream and surface Ekman layer is balanced by southward flow of less salty deep waters, transports freshwater southward at a rate of about 0.4 Sv at 26°N. The AMOC freshwater transport when added to the Bering Strait throughflow of 0.8 Sv results in a total southward freshwater transport of 1.2 Sv across 26°N. On long time scales, the northward salinity transport across 26°N associated with the AMOC is balanced by the freshening of the northern Atlantic waters due to net precipitation and river inflows that result in the southward transport of freshwater at 26°N. Variations in the AMOC are strongly correlated with variations in freshwater transport at 26°N with the AMOC accounting for 90% of the variations in freshwater transport. The remaining 10% of the northward salinity transport is again contributed by the horizontal gyre circulation. McDonagh et al. estimated that a 1-Sv decline in the AMOC decreases the southward freshwater transport (or increases the northward freshwater transport) by 0.047 Sv. For the 2.5-Sv reduction in the AMOC from pre-2009 values to post-2009 values, we expect a reduction in southward freshwater transport of 0.11 Sv at 26°N. In fact, the average freshwater transport from 2004 to 2009 was −1.24 Sv and the average ocean freshwater transport from 2009 to 2016 after the 2.5-Sv reduction in the AMOC was −1.13 Sv (Fig. 3), corresponding to a reduction in southward freshwater flux across 26°N of 0.12 Sv. This reduction in southward freshwater flux is equivalently an increase in northward freshwater flux of 0.12 Sv and for clarity we will describe the change as an increase in northward freshwater transport across 26°N from before 2009 to after 2009.

Based on the variability in annual average values for the MOC given in Smeed et al. (2018, their supplemental Table S1) and for heat and freshwater transports given in Figs. 2 and 3, changes of all variables from before 2009 to after 2009 represent significant differences. The change from before 2009 to after 2009 in the MOC is 2.5 Sv with an estimated standard error of ±0.8 Sv;
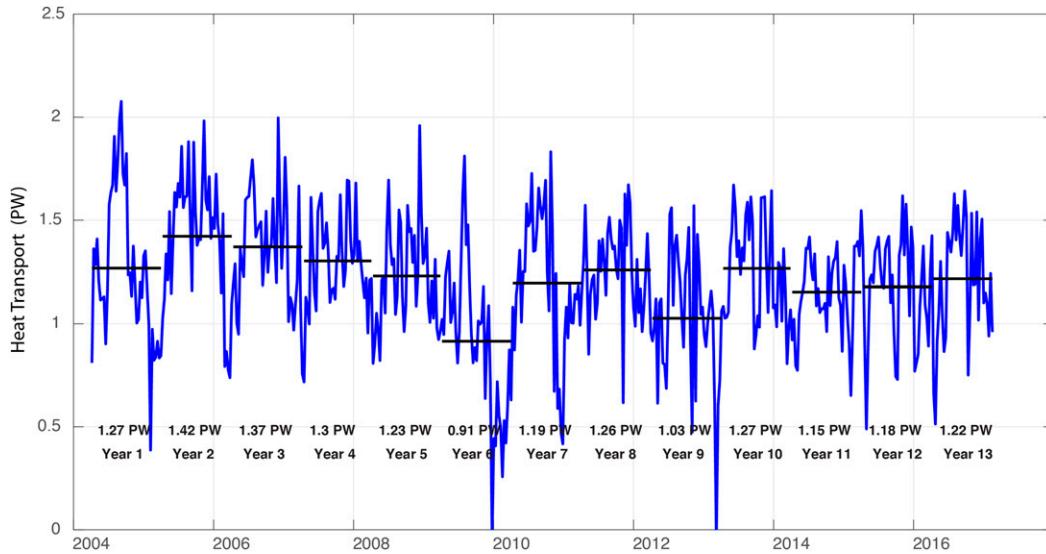
FIG. 2. Ocean heat transport at 26°N from RAPID measurements. Ten-day filtered values following the method in Johns et al. (2011) are shown. Horizontal black lines indicate annual average values (April–March) for each year. Northward ocean heat transport averages 1.32 PW for 2004–09 but only 1.15 PW after 2009. There is a decrease in ocean heat transport of 0.17 PW resulting from the reduction in the AMOC during late 2008 and early 2009.

the change in heat transport is 0.17 ± 0.06 PW and in freshwater transport is 0.12 ± 0.04 Sv. In each case the difference is significant at a 95% confidence level being more than 2 times the standard error.

Overall, for the period after 2009, the AMOC is 13% (2.5 Sv) smaller, the northward ocean heat transport across 26°N is 13% (0.17 PW) smaller and the northward freshwater transport is 10% (0.12 Sv) larger than they were for the 5-yr period April 2004 to March 2009. What are the effects of a persistent 13% reduction in the AMOC over an 8-yr period? In this analysis, we will use the changes in ocean heat and freshwater transports
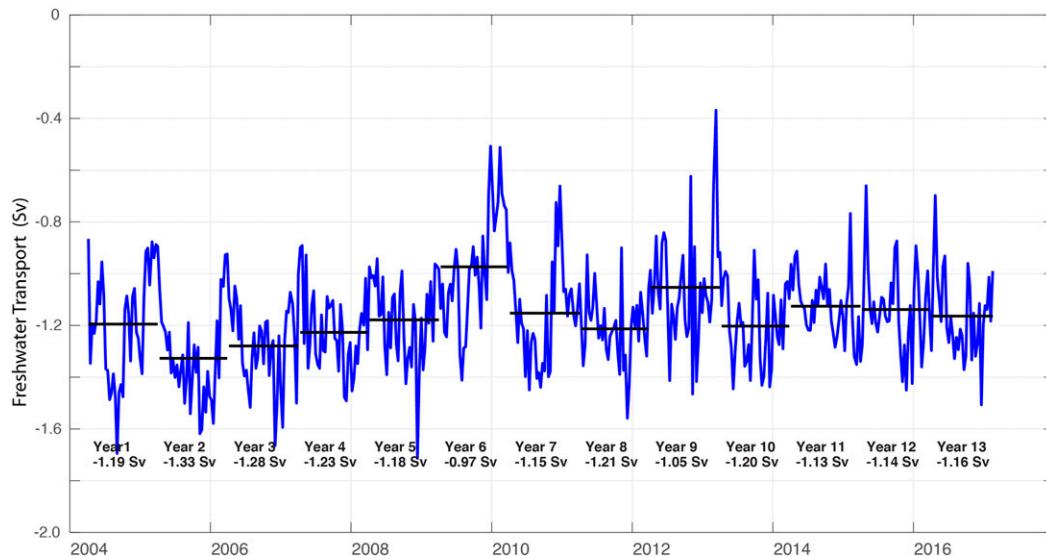

FIG. 3. Freshwater transport across 26°N from RAPID measurements. Ten-day filtered values following the method in McDonagh et al. (2015) are shown. Horizontal black lines indicate annual average values (April–March) for each year. Southward freshwater transport during 2004–09 averages 1.24 Sv. As a result of the reduction in the AMOC in late 2008 and early 2009, southward freshwater transport after 2009 averages only 1.13 Sv. There is an increase in northward freshwater transport across 26°N of 0.12 Sv from before 2009 to after 2010.

observed at 26°N to examine how the 2.5-Sv reduction in the AMOC from pre-2009 to post-2009 values affects the temperature and salinity structure of the North Atlantic north of 26°N.

3. Effects of changes in ocean heat transport and ocean freshwater transport

For the ocean basin north of 26°N that is nearly closed except for the small inflow through the Bering Strait, changes in ocean heat transport at 26°N Δ(MHT) must be balanced either by a change in ocean heat content (OHC) in the basin north of 26°N Δ(OHC)/Δt or by changes in air–sea heat flux Δ(ASHF) so that

$$\Delta(\text{MHT}) = \Delta(\text{OHC})/\Delta t + \Delta(\text{ASHF}). \qquad (1)$$

Similarly changes in freshwater transports at 26°N Δ(FWT) must be balanced either by changes in ocean freshwater content (OFWC) in the basin north of 26°N Δ(OFWC)/Δt or by changes in precipitation minus evaporation $\Delta(P - E)$:

$$\Delta(\text{FWT}) = \Delta(\text{OFWC})/\Delta t + \Delta(P - E). \qquad (2)$$

The meridional heat transport time series at 26°N includes a constant 0.8-Sv inflow from the Pacific to the Atlantic through the Bering Strait at 0°C and the meridional freshwater transport time series at 26° includes a southward freshwater transport associated with a 0.8-Sv flow through the Bering Strait with a salinity of 32.5.

In practical terms, we consider balances 1 and 2 for the closed ocean region between 26° and 70°N because there are few observations of heat and freshwater content north of 70°N and because observations suggest that ocean heat transport variability at 70°N is small (Østerhus et al. 2005; Hansen et al. 2008, 2016; Jochumsen et al. 2017) and we believe that the variations in ocean freshwater transport relative to constant Bering Strait throughflow are also small at 70°N. We seek first to assess the effects of a reduction in northward ocean heat transport and an increase in northward ocean freshwater flux across 26°N from before 2009 to after 2009 on the temperature and salinity in the ocean region between 26° and 70°N using the "EN4" climatology of temperature and salinity profiles (Good et al. 2013). The EN4 climatology in the North Atlantic since 2004 is largely based on free-drifting Argo float profiles that are designed to sample every 10 days at spatial intervals of about 300 km. Because the ocean exhibits large variability on eddy scales of 100 km or less, the EN4 estimates of ocean heat and freshwater content have large temporal and spatial variability. To dampen this variability, we first calculated
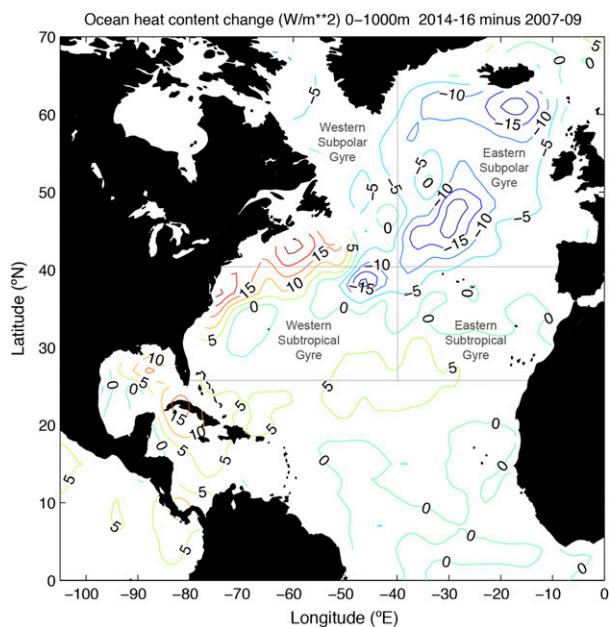

FIG. 4. Ocean heat content change (W m^{-2}) for 2014–16 minus 2007–09. EN4 gridded temperature and salinity fields updated from Good et al. (2013) are used.

annual average heat content change and freshwater content change from 2008 annual average values. We use the 2008 annual averages as a baseline for the state of the ocean before the 2.5-Sv reduction in the AMOC in late 2008 or early 2009. The changes from 2008 baseline values indicate the effects of the AMOC reduction on the temperature and salinity structure north of 26°N.

We first calculated annual average heat content change, Δ(OHC)/dt, from baseline 2008 values on the 1° × 1° EN4 grid and examined the spatial variability on annual maps. Heat content change is defined here as the difference between annual average potential temperature minus 2008 average potential temperature integrated over depth from the surface to 1000-m depth and multiplied by density and specific heat ($\rho C_p = 4 \times 10^7 \, \text{J m}^{-3}\,^\circ\text{C}^{-1}$). Dividing by the number of years, Δt, since 2008 then produces local estimates of ocean heat content change in watts per square meter. Integrating these heat content changes over the ocean region 26° to 70°N produces estimates of overall heat content change north of 26°N in petawatts.

We found the annual maps of ocean heat content change to be too noisy to interpret coherently. Even 2-yr maps are noisy though patterns begin to emerge. To illustrate the overall pattern in ocean heat content change, we use 3-yr averages to show the map of 2014–16 average heat content minus 2007–09 average heat content (Fig. 4). For the 8-yr period from April 2009 to February 2017, the

TABLE 1. Time changes in ocean heat and freshwater content for 26°–70°N over intervals of 2, 4, and 8 years to show consistency of ocean heat and freshwater content change. EN4 gridded temperature and salinity fields updated from Good et al. (2013) are used.

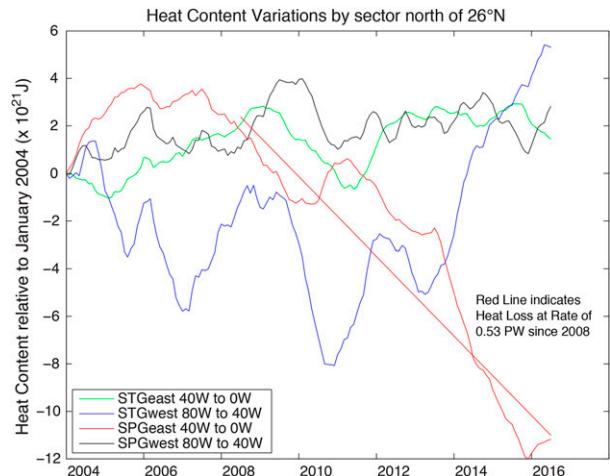| Interval	Period	Heat content change (PW)	Freshwater content change (Sv)
8 years	2016–08	−0.037	0.062
4 years	2012–08	−0.026	0.040
	2016–12	−0.048	0.084
2 years	2010–08	−0.039	0.069
	2012–10	−0.012	0.010
	2014–12	−0.060	0.159
	2016–14	−0.035	0.008

FIG. 5. Temporal variability in ocean heat content north of 26°N for four regions: Subtropical Gyre East (26°–40°N, 40°W–0°), Subtropical Gyre West (26°–40°N, 80°–40°W), Subpolar Gyre East (40°–70°N, 40°W–0°), and Subpolar Gyre West (40°–70°N, 80°–40°W). Differences from 2004 values are shown for each region. EN4 gridded temperature and salinity fields updated from Good et al. (2013) are used. The red line indicates ocean heat loss at a rate of 0.053 PW based on a least squares estimate of the slope in heat content change since 2008. Estimated uncertainty in this change for Subpolar Gyre East is 0.018 PW, assuming independent values every 12 months.

RAPID time series of ocean heat transport shows a heat transport that is 0.17 PW lower than for the period from April 2004 to April 2009. Hence we are looking for a change in ocean heat content of order 0.1 PW using 2007–09 as a baseline. The 2014–16 minus 2007–09 map of ocean heat content change (Fig. 4) shows cooling of the ocean north of 26°N in a pattern where the largest cooling broadly follows the offshore, southeastern edge of the Gulf Stream Extension/North Atlantic Current. Such pattern is consistent with our interpretation that more of the Gulf Stream flow is recirculating southward and less warm water is penetrating northward in the North Atlantic Current into the subpolar gyre. The largest cooling, on the order of $20 \, \mathrm{W \, m^{-2}}$, occurs in the midocean at about 48°N, 30°W.

We have repeated the calculations and maps at 4-yr intervals, 2012–08 and 2016–12, and the patterns are similar (though noisier) with similar cooling of the northern Atlantic at rates of 0.03 (2012–08) and 0.05 PW (2016–12). We have also estimated the overall cooling at 2-yr intervals with the results (Table 1) showing that there has been constant cooling throughout the 8-yr period in agreement with the sustained reduction in ocean heat transport across 26°N. The northern Atlantic has cooled significantly and consistently since 2008 in a pattern where the changes in heat content are aligned along the course of the Gulf Stream Extension/North Atlantic Current. The pattern in ocean heat content change also shows warming along the western boundary. This overall pattern of warming near the coast and cooling along the path of the North Atlantic Current is reminiscent of the pattern found by Zhang (2008) in a modeling study for the "fingerprint" of an increase in the AMOC. For an increase in AMOC, there was cooling near the coast and warming along the path of the North Atlantic Current, opposite to what we observe here for a reduction in the AMOC since 2008. The integrated change in ocean heat content considering the

entire region from 26° to 70°N is 0.04 PW (Table 1), a factor of 4 less than the 0.17 PW change in ocean heat transport across 26°N.

To achieve better temporal resolution, we have calculated annual average heat content relative to January 2004 values on the 1° × 1° EN4 grid for each month from 2004 to 2016 by averaging 12 monthly values. These heat content changes are then summed up over four regions indicated in Fig. 4: the 1) western subtropical gyre, 26°–40°N, 80°–40°W, 2) eastern subtropical gyre, 26°–40°N, 40°W–0°, 3) western subpolar gyre, 40°–70°N, 80°–40°W, and 4) eastern subpolar gyre, 40°–70°N, 40°W–0° (Fig. 5). The results show that almost all of the cooling since April 2009 has occurred in Subpolar Gyre East at a rate of −0.053 PW, with some warming in Subtropical Gyre West (0.027 PW) and little change in heat content over Subpolar Gyre West (−0.002 PW) and Subtropical Gyre East (−0.006 PW). The cooling in Subpolar Gyre East is significant as estimated from the slope of the heat content change from 2008 to 2016 (0.053 ± 0.018 PW) with the uncertainty based on the assumption that 12-month heat content values are independent. Integrating the heat content change over the region 26°–70°N produces an overall cooling of the northern Atlantic Ocean between 26° and 70°N at a rate of 0.04 PW from 2008 to
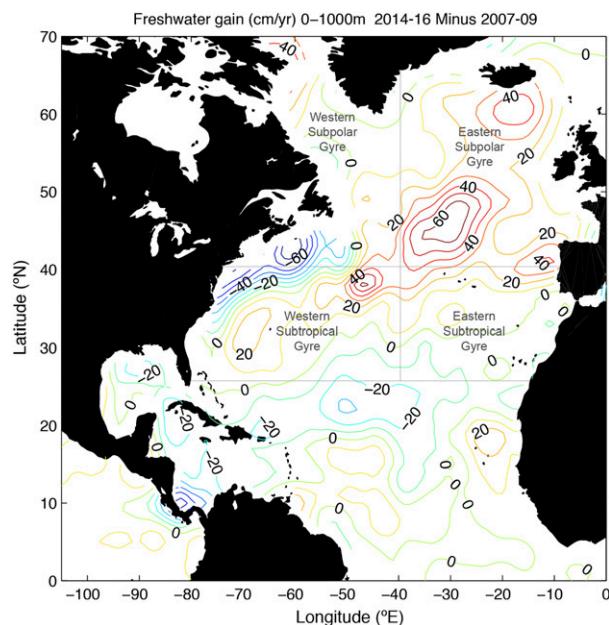
FIG. 6. Ocean freshwater content change (cm yr^{-1}) for 2014–16 minus 2007–09. EN4 gridded temperature and salinity fields updated from Good et al. (2013) are used.

2016. The reduction in ocean heat transport across 26°N in late 2008 or early 2009 shows up in a consistent 0.05 PW cooling of the eastern subpolar gyre north of 40°N and east of 40°W (Fig. 5).

We have done a similar analysis of changes in freshwater content north of 26°N since 2008, Δ(OFWC)/Δt, that we associate with the 2.5-Sv reduction in the AMOC from before 2009 to after 2009. Effectively the reduced AMOC is transporting a smaller amount of salty upper subtropical waters northward after 2009. We estimate the patterns of freshwater content change from 2008 values by taking the difference in salinity on the 1° × 1° EN4 grid, integrating from the surface to 1000-m depth and dividing by −35 "practical salinity units." Dividing by the number of years since 2008 produces local estimates of freshwater content change in centimeters per year. The spatial pattern in freshwater content change 2014–16 minus 2007–09 is similar to the pattern of ocean heat content change with largest freshening on the offshore, southeastern side of the Gulf Stream and North Atlantic Current and some higher salinities along the east coast of North America (Fig. 6). Freshening is largest in midocean at about 48°N, 30°W reaching values of 60 cm yr^{-1}. Integrating the freshening over the ocean region from 26° to 70°N produces a freshening at the rate of 0.062 Sv (ΔOFWC/Δt), more than 50% of the change in freshwater transport of 0.12 Sv (ΔFWT) at 26°N associated with the 2.5-Sv reduction in the AMOC. Freshening
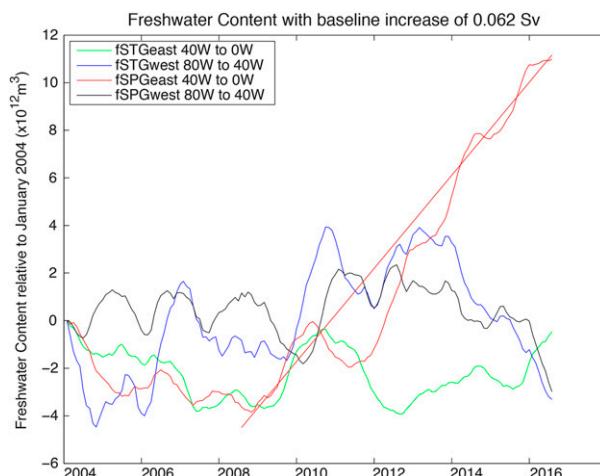

FIG. 7. Temporal variability in ocean freshwater content north of 26°N for four regions: Subtropical Gyre East (26°–40°N, 40°W–0°), Subtropical Gyre West (26°–40°N, 80°–40°W), Subpolar Gyre East (40°–70°N, 40°W–0°), and Subpolar Gyre West (40°–70°N, 80°–40°W). Differences from 2004 values are shown for each region. EN4 gridded temperature and salinity fields updated from Good et al. (2013) are used. The red line indicates an increase in ocean freshwater at a rate of 0.062 Sv based on a least squares estimate of the slope in freshwater content change since 2008 in the eastern subpolar gyre. Estimated uncertainty in this change for Subpolar Gyre East is 0.013 Sv, assuming independent values every 12 months.

over 4-yr intervals 2016–12 and 2012–08 (Table 1) shows freshening consistent with a constant reduction in the AMOC since 2009.

The same regional analysis for the annual averaged freshwater content as performed for ocean heat content shows that almost all of the freshening since April 2009 has occurred in Subpolar Gyre East at a rate of +0.062 Sv, with some decrease in freshwater content in Subpolar Gyre West (−0.01 Sv) and little change in freshwater content over Subtropical Gyre West and Subtropical Gyre East (Fig. 7). The freshening in Subpolar Gyre East is significant as estimated from the slope of the freshwater content change from 2008 to 2016 (0.062 ± 0.013 Sv), with the uncertainty based on the assumption that 12-month freshwater content values are independent. The increase in northward freshwater transport across 26°N in late 2008 or early 2009 shows up in a consistent 0.062-Sv freshening of the eastern subpolar gyre north of 40°N and east of 40°W since 2008. Thus, the major changes in ocean heat content (ΔOHC)/Δt and ocean freshwater content (ΔOFWC)/Δt associated with the reduced northward ocean heat transport (ΔMHT) and increased northward freshwater transport (ΔFWT) across 26°N since 2008 occur in the eastern subpolar gyre north of 40°N and east of 40°W.

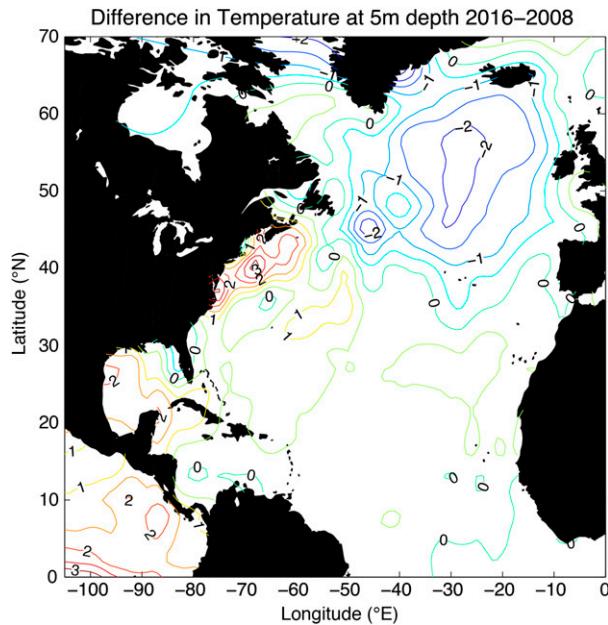## Difference in Temperature at 5m depth 2016–2008

FIG. 8. Difference in temperature at 5-m depth (2016 minus 2008) based on EN4 annual average temperatures updated from Good et al. (2013). Surface temperatures are 2°C colder over 8 years in the midocean region south of Iceland.

4. Character of the cooling of the subpolar gyre

A dramatic manifestation of the cooling in the subpolar gyre is the emergence of the "cold blob," or "warming hole," in sea surface temperature south of Greenland–Iceland. The cold blob has emerged in maps of global warming, and its cause has been attributed to the slowing AMOC (Drijfhout et al. 2012; Rahmstorf et al. 2015; Sévellec et al. 2017). In model projections of future climate change it is common to see a cold blob south of Greenland–Iceland that is widely assumed to be related to the slowdown in model AMOC over the twenty-first century. Here we show the difference in annual average 5-m depth temperature from 2008 to 2016 in the EN4 climatology (Fig. 8). Near-surface temperatures are more than 2°C colder in 2016 after 8 years of reduced AMOC. It is important to appreciate that these are changes in annual average values, the cooling persists year-round, and the cooling continues down into the thermocline so that the annual average temperature at 500-m depth in some areas of the eastern subpolar gyre is more than 2°C colder in 2016 than it was in 2008.

Examining the annual average potential temperature profiles for 2008 and 2016 from EN4 at 48°N, 30°W, we see that 2016 temperatures are about 2°C colder than 2008 temperatures from the surface down to 800-m depth (Fig. 9). A vertical uplift of the thermocline
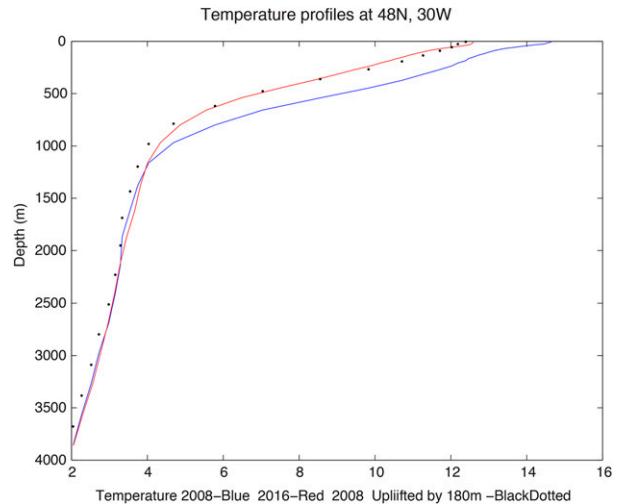
Temperature profiles at 48N, 30W

FIG. 9. Temperature profiles at 48°N, 30°W in 2008 (blue) and 2016 (red) based on EN4 data updated from Good et al. (2013). The black dots indicate 2008 profile uplifted by 180 m to show that the thermocline in the eastern subpolar gyre has risen since 2008.

from 2008 to 2016 by about 180 m (as shown by the dotted curve in Fig. 9) can explain much of the cooling. We have also estimated the average temperature profiles over 40°–70°N, 40°W–0° for 2008 and 2016 to show that the cooling is widespread: for this area average, temperatures are 0.6°C cooler in 2016 down through the thermocline to 800-m depth and there is an average upward displacement of isotherms in the main thermocline by about 90 m. (Fig. 10). Similar averages for salinity indicate an uplift of the halocline and widespread freshening of the eastern subpolar gyre where 2016 salinities are 0.07 lower than 2008 salinities down through the thermocline.

The explanation for these changes in the eastern subpolar gyre derives from the changes in circulation associated with the reduction in the AMOC from before 2009 to after 2009. As noted earlier, the increased thermocline recirculation in the subtropical gyre combined with no change in the Gulf Stream and the decreased southward flow of LNADW indicates that there is less northward transport of warm, salty upper waters across the boundary between the subtropical and subpolar gyres at roughly 40°N and less southward transport of cold, fresher deep waters across this boundary. In a quasi-two-layer interpretation, we expect the thermocline separating the warm upper and cold deeper waters in the subpolar gyre north of 40°N to rise so that there is less upper water above the thermocline and more deep water below the thermocline. We examined the displacement of the 8°C isotherm (which is in the main thermocline throughout the entire subtropical gyre and

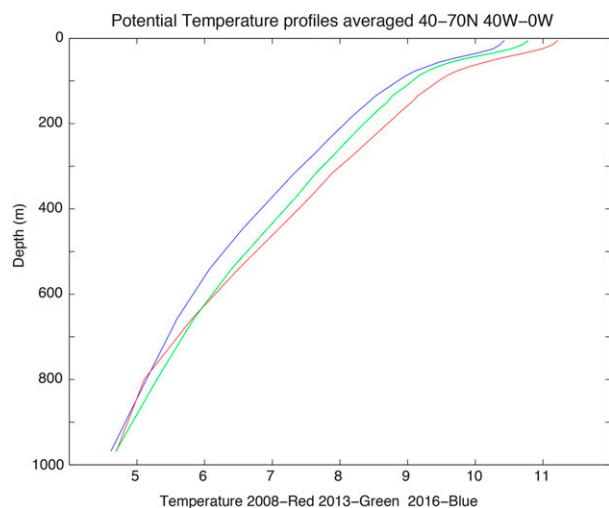Potential Temperature profiles averaged 40–70N 40W–0W

FIG. 10. Potential temperature profiles. Annual average temperatures from EN4 updated from Good et al. (2013) are averaged over the eastern subpolar region 40°–70°N, 40°W–0° for 2008, 2013, and 2016 to show persistent cooling from 2008 to 2016. Here, 2013 is chosen because it is before the severe winters of 2014 and 2015 and it indicates cooling since 2008 down to 650 m. The severe winter mixing in 2014 and 2015 led to cooling down to 800 m.

much of the eastern subpolar gyre) and find that the 8°C isotherm has moved upward from 2008 to 2016 by more than 100 m in the eastern subpolar gyre. This upward heave produces colder and fresher waters at all depths above 1000-m depth that are reflected in the observed changes of ocean heat (and freshwater) content. The spatial pattern in heave of the 8°C isotherm is similar to the pattern in heat content change (Fig. 4).

5. Changes in air–sea heat exchange

On interannual time scales, the ocean heat transport across 26°N in the Atlantic should be balanced by the combination of ocean heat content change and air–sea heat exchange north of 26°N according to Eq. (1). The RAPID observations provide us with a time series of ocean heat transport (Fig. 2) and the EN4 climatology provide estimates of ocean heat content change. Subtracting ocean heat content change from ocean heat transport then provides an ocean-based estimate of air–sea heat flux (ASHF) for the Atlantic Ocean north of 26°N (Fig. 11). These are effectively annual average values being running means over 12 months. Johns et al. (2011) estimated the uncertainty in annual average heat transport at 26°N to be 0.13 PW. We estimate the uncertainty in annual average heat content change to be 0.10 PW based on the residuals from the linear fit for ocean heat content variations from 26° to 70°N from 2008 to 2016. Thus, the uncertainty in our estimate of

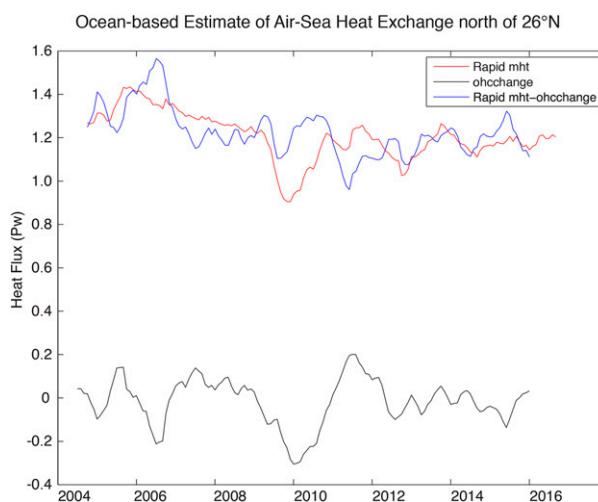Ocean-based Estimate of Air-Sea Heat Exchange north of 26°N

FIG. 11. Ocean heat transport at 26°N (red), ocean heat content change (black), and their sum (blue), which is equal to the ocean heat loss to the atmosphere north of 26°N. The sum represents an ocean-based estimate of ocean heat loss for the Atlantic between 26° and 70°N.

annually averaged air–sea heat exchange north of 26°N is 0.17 PW under the assumption that the uncertainties in heat transport and heat content change are uncorrelated.

From Fig. 11, we see that the reduction in ocean heat transport at 26°N during the 2009–10 event is largely balanced by a cooling of the region north of 26°N, with little effect on the air–sea heat flux that is the sum of ocean heat transport and ocean heat content change. On longer time scales we have shown that part of the reduction by 0.17 PW in ocean heat transport across 26°N from before 2009 to after 2009 can be accounted for by an overall cooling of the North Atlantic at a rate of 0.04 PW from 2008 to 2016. Thus our ocean-based estimates of air–sea heat exchange indicate a reduction in ocean heat loss north of 26°N of 0.12 PW for the period after 2008. We next examine whether similar changes in the amount of air–sea heat exchange are exhibited in available surface heat flux climatologies for the region north of 26°N after 2008. It is expected that the ocean would give up less heat to the atmosphere after 2008 because of the cooler ocean surface temperatures in the North Atlantic and particularly in the eastern subpolar gyre. But do the climatological estimates show such a reduction?

We first examined Trenberth and Fasullo's (2017, hereinafter TF17) estimates of air–sea heat flux north of 26°N based on their conclusion that their new fluxes were superior to traditional climatologies. TF17 made these new estimates of air–sea heat exchange by first estimating the net radiation at the top of the atmosphere
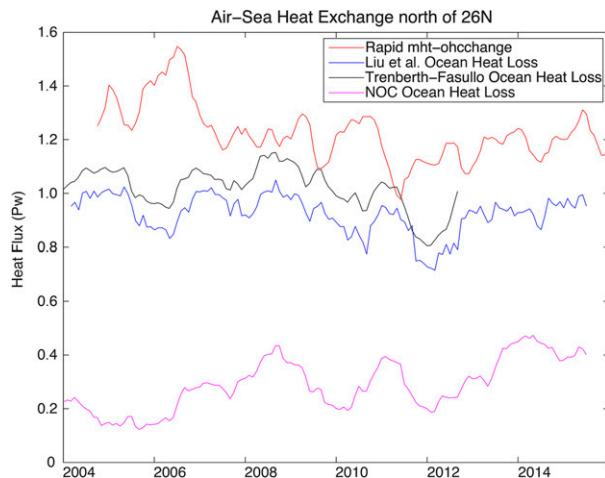
FIG. 12. Comparison of ocean-based estimates of ocean heat loss north of 26°N with recent climatologies of air–sea exchange. The ocean-based estimate from Fig. 11 is equal to the northward heat transport at 26°N from RAPID measurements minus ocean heat content change north of 26°N from EN4 values for heat content; J. Fasullo provided the ocean heat loss estimates from TF17, C. Liu provided the values of ocean heat loss from L17, and E. Kent provided the NOC ocean heat loss based on ship of opportunity measurements [updated from Berry and Kent (2011)].

on a point-wise basis and then subtracting the divergence of atmospheric energy transport using the ERA-Interim reanalysis which they asserted were the best available. Their time series of air–sea heat fluxes north of 26°N (shown in Fig. 12) indicated that there was little change in air–sea flux during the 2009–10 event, in agreement with our estimates. For the longer time period, there is a difference between TF17's air–sea fluxes before 2009 and after 2009. Their time series shows a drop in heat loss from the ocean to the atmosphere north of 26°N from 1.06 PW for the period from April 2004 to March 2009 to 0.96 PW for the period from April 2009 to December 2013. Thus, TF17's estimates of air–sea heat exchange suggest that the air–sea heat exchange north of 26°N is reduced by 0.10 PW after 2009. We also examined the estimates of air–sea heat exchange from Liu et al. (2017, hereinafter L17) in Fig. 12. L17 use a similar analysis method to TF17 and their estimates closely track those of TF17 but with slightly lower values. Their estimates also show little change in air–sea flux during the 2009–10 event but show an ocean heat loss north of 26°N for the period from April 2009 to March 2015 that is 0.07 PW smaller than for the period from April 2004 to March 2009.

The ocean-based estimates of air–sea heat exchange can provide a useful comparison with other air–sea exchange climatologies. Note that both the TF17 and L17 ocean heat losses (Fig. 12) are less than implied by

our ocean-based estimate of ocean heat loss (MHT + ΔOHC/Δt), but both are closer to our ocean heat loss than traditional products [MERRA, ERA, JRA, NCEP, and National Oceanography Centre (NOC)]. NOC values are shown in Fig. 12; ERA, MERRA, JRA, and NCEP values are higher than NOC but still substantially below our ocean-based estimates and those of TF17 and L17. Here we are primarily considering changes in ocean heat loss over time, and the TF17 and L17 calculations agree with our new ocean-based estimate of air–sea exchange that there was little change in air–sea exchange during the 2009–10 event and that there is a reduction in ocean heat loss north of 26°N after 2008.

If we add our estimate of the reduction in ocean heat content Δ(OHC) north of 26°N of 0.04 PW to the order 0.10 PW in reduced ocean heat loss found by TF17 and L17, we can account for 0.14 PW, which is most of the 0.17 PW change in ocean heat transport Δ(MHT) across 26°N from the period before April 2009 to the period after March 2009. Most interesting is that the air–sea exchange appears to have adjusted to the sharp change in the AMOC and associated change in ocean heat transport on a relatively short interannual time scale.

To examine the pattern of change in air–sea heat exchange from before 2009 to after 2009, we examined the NOC air–sea heat flux climatology based on ship observations of air and sea temperatures, wind speed and humidity (Berry and Kent 2011). We took the difference in the NOC net heat flux, 2011–15 average minus 2004–08 average (Fig. 13). There is a broad region of decreased net ocean heat loss extending southwest to northeast from the Bahamas toward Iceland with differences as large as 20 W m^{-2}. Error maps for 5-yr average NOC heat fluxes indicate uncertainties of order 5 W m^{-2} in this region that is well sampled by ships of opportunity [Berry and Kent (2011), updated to 2015], so we consider these decreased ocean heat losses to be significant. This pattern corresponds roughly to the region of ocean heat loss and freshwater gain seen in Figs. 4 and 6 and accords with the general idea that the ocean heat loss should decrease when upper-ocean surface temperatures get colder. Summing up the change in air–sea heat exchange over this coherent region of change yields a reduction in ocean heat loss of 0.10 PW similar to the change in TF17's and L17's air–sea heat fluxes. This pattern of reduced ocean heat loss to the atmosphere in the coherent region stretching from the Bahamas to Iceland where ocean heat content has decreased suggests that the air–sea heat exchange has been affected by the reduction in ocean heat transport at 26°N.

The map of 2011–15 minus 2004–08 net air–sea heat flux for the NOC climatology exhibits an increase in ocean heat loss along the western boundary and into the
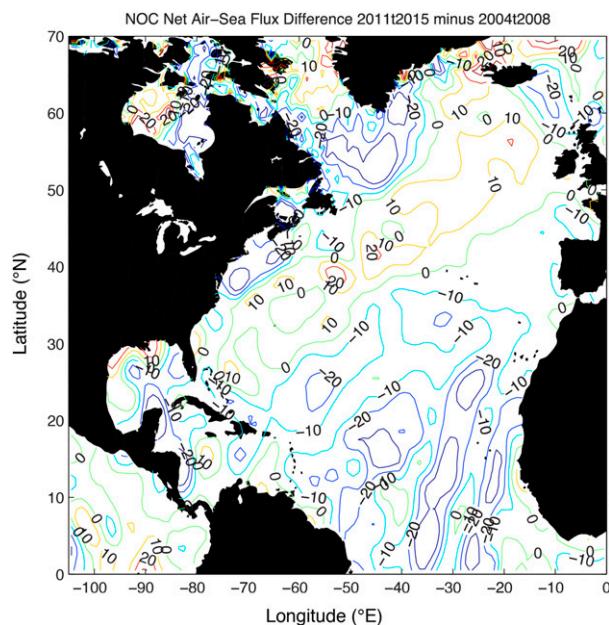
FIG. 13. Air–sea exchange difference (2011–15 average minus 2004–08 average) for the NOC air–sea flux climatology. Positive values represent less ocean heat loss in the later period. Uncertainty maps from Berry and Kent (2013) suggest that uncertainties in 5-yr ocean heat loss are about $5\,\mathrm{W\,m^{-2}}$ in the well-sampled region stretching from Florida toward Iceland.

Labrador Sea so that the overall change in ocean heat loss to the atmosphere north of 26°N in the NOC climatology is actually an increase in ocean heat loss at a rate of 0.09 PW (Fig. 12). Other climatologies (MERRA, ERA, JRA, and NCEP) show a similar increase in ocean heat loss (2011–15 minus 2004–08). Hence NOC and other traditional climatologies actually suggest increased ocean heat loss over the ocean north of 26°N from 2004–08 to 2011–15. Therefore there is a discrepancy between overall surface heat flux trends in the bulk-formula-derived climatologies (NOC, MERRA, ERA, JRA, and NCEP) and those derived from "residual" methods (TF17; L17). Nevertheless, the coherent pattern of reduced ocean heat loss to the atmosphere in the region stretching from the Bahamas to Ireland (Fig. 13) suggests that the air–sea heat exchange has been affected by the reduction in ocean heat transport at 26°N.

6. Discussion and conclusions

The suggested long-term decline in the AMOC from 1957 to 2004, the reduction in the AMOC during 2009–10, and the long-term reduction in the AMOC from before 2009 to after 2009 are all associated with reduction in the southward flow of Lower North Atlantic Deep Water below 3000-m depth and with a compensating increased southward recirculation of upper thermocline waters within the subtropical gyre. The 2009–10 event and the reduction in the AMOC in late 2008 or early 2009 represent relatively short-term changes relative to the low-frequency decadal variations in the North Atlantic Oscillation or Atlantic multidecadal variability (AMV) that are generally considered. Because of the difference in time scale we do not attempt to attribute these relatively abrupt Atlantic changes to low-frequency variations in the global climate system. Instead we view these abrupt changes in the AMOC as triggers for low-frequency variations like those of the AMV. In a study of long-term variations in the subpolar gyre of the North Atlantic, Chafik et al. (2016) showed that variations in subpolar North Atlantic temperature have profound effects on the global climate system including the Walker circulation and Pacific decadal variability. In their language, the subpolar North Atlantic is in a phase transition from a warm state to a cold state since the sharp reduction in the AMOC in 2009. In our view this phase transition could be triggered by the sharp reduction in AMOC. Here we focus on the effects of changes in AMOC on the recent evolution of temperature and salinity in the Atlantic Ocean north of 26°N and particularly in the subpolar gyre. These results suggest that rapid changes in the AMOC affect the longer-term (decadal) variability in the subpolar North Atlantic that may connect with Pacific variability as suggested by Chafik et al. (2016).

Because we observe almost no change in the Gulf Stream flow through the Straits of Florida and Rossby et al. (2014) maintained that there are no changes in Gulf Stream transport across the New York to Bermuda section, we think that the relatively constant Gulf Stream along the western boundary persists to a latitude of about 40°N at which latitude more of the Gulf Stream waters turn to recirculate southward (Schmitz and McCartney 1993) after 2009. With less northward transport of warm, salty upper waters across 40°N and less southward transport of cold, fresher deep waters across 40°N, the waters of the subpolar gyre become colder and fresher and the thermocline separating the upper and deeper waters rises in the subpolar gyre north of 40°N. This uplift of the thermocline, often called heave, is sometimes discounted as a reversible oscillation in water mass structure. But in the northern Atlantic where deep wintertime mixing exposes the deep thermocline waters to the surface during severe winters, the uplift of the thermocline means that uplifted colder, fresher waters are available to be mixed to the surface. The upward displacement of the thermocline puts cold waters closer to the sea surface throughout the year so when a severe winter comes

along and mixes the colder deep waters up to the surface, sea surface temperatures become dramatically colder.

For the eastern subpolar gyre, we see these processes in the evolution of potential temperature profiles (Fig. 10). From 2008 to 2013, there is progressive cooling of the upper 600 m of the water column that is due to the reduced northward flow of warm upper waters into the subpolar gyre. In January–February 2014 and again in 2015, there were strong wintertime events that mixed the upper 800 m of the water column (Grist et al. 2016; Josey et al. 2018) so that the colder 2016 temperatures penetrate down to 800-m depth. The combination of the preconditioning of the subpolar gyre toward cooler temperatures after 2008 with the vigorous deep wintertime mixing during 2014 and 2015 leads to cooler temperatures all the way down to 800-m depth.

Josey et al. (2018) attributed the cold blob after 2015 primarily to the dramatic wintertime heat loss event in 2014–15 that led to deep mixing. In fact, the preconditioning of the subpolar gyre with upward heave of the thermocline after 2008 had already put cold waters closer to the sea surface throughout the year, so the severe wintertime heat losses in 2014 and 2015 led to the creation of very cold (and fresh) surface waters after the winter of 2015, the location of which is determined largely by where the deepest wintertime mixing occurred. The intensity of the cold blob reflects the preconditioning of the subpolar gyre toward colder, fresher waters in the upper thermocline resulting from the reduced northward heat and salinity transport since 2008 while the location of the cold blob reflects where the dramatic wintertime mixing was strongest.

Our results therefore indicate that the cooling in the eastern subpolar gyre and the evolution of the cold blob are fundamentally linked to the reduced ocean heat transport at 26°N. While ocean heat transport, ocean heat content change and air–sea heat exchange represent a balance as shown by Eq. (1), the reduced ocean heat loss to the atmosphere found here and by TF17 and L17 would have led to a warming of the ocean north of 26°N in the absence of the reduction in ocean heat transport. Hence we maintain that the cooling of the eastern subpolar gyre and the reduced ocean heat loss to the atmosphere are both due to the reduced ocean heat transport at 26°N.

Quantitatively, freshwater transport changes at 26°N more closely agree with the time changes in freshwater content north of 26°N while ocean heat transport changes are substantially larger than observed changes in ocean heat content. This is possibly due to the more direct feedback between ocean surface temperatures and the air–sea heat exchanges. Colder ocean surface temperatures mean less ocean heat loss (in the absence of wind changes) so that ocean temperatures do not decrease as much as the changes in ocean heat transport would suggest because of the feedback with the air–sea exchanges. For freshwater, we do not expect a change in air–sea freshwater exchange (evaporation and precipitation) for small changes in ocean surface salinity so there is not a direct feedback. Changes in air–sea freshwater water exchanges may be more closely aligned with changes in surface temperature changes in that lower ocean surface temperatures are expected to result in less evaporation which would lead to freshening of the surface waters. The role of precipitation changes is more difficult to assess. Thus, the closer agreement between freshwater transport changes at 26°N and observed changes in freshwater content north of 26°N is likely the result of a lack of a direct feedback between surface salinity changes and air–sea freshwater exchange.

Changes in upper-ocean temperature may affect the atmosphere beyond reducing the amount of ocean heat loss to the atmosphere. It has been argued that the cold blob in sea surface temperature is associated with a high pressure region in the atmosphere particularly in summer that leads to warmer than normal summers over the United Kingdom and northwestern Europe (Haarsma et al. 2015; Duchez et al. 2016). It is intriguing to speculate that the strengthening cold blob led to the record warm, dry summer of 2018 over the United Kingdom. That such a summer may result from the weakening of the AMOC 10 years earlier and the cumulative cooling of the North Atlantic subpolar gyre suggests that the ocean could have a major role in summer seasonal predictions over northwestern Europe.

Combining ocean heat transport with ocean heat content change to produce ocean-based time series of air–sea heat exchange offers a powerful method for evaluating the accuracy of air–sea heat flux climatologies. The method without considering time changes in ocean heat content has been used for many years for evaluating climatological estimates of air–sea fluxes (Bryden 1993). Here we suggest that ocean-based estimates of air–sea fluxes can be used not just for climatological estimates but also to assess the accuracy of temporal variations in air–sea fluxes, especially those derived in new climatologies (Fig. 12). For the TF17 and L17 estimates of air–sea fluxes (Fig. 12), we see a closer agreement in the overall magnitude between the ocean-based estimates and the new climatologies than has traditionally been the case for bulk-formula climatologies like NOC (Fig. 12). More striking is that the decadal variations in both the ocean-based estimate and the new climatology values have similar magnitudes. Combining new Overturning in the Subpolar North

Atlantic Program (OSNAP) estimates of ocean heat transport across a subpolar latitude of about 58°N (Lozier et al. 2019) with the ongoing RAPID estimates of ocean heat transport at 26°N, we will soon be able to compare ocean-based estimates of air–sea fluxes with climatological estimates of air–sea exchange for the subtropical–subpolar region between 26° and 58°N on a continuing basis.

REFERENCES

Berry, D. I., and E. C. Kent, 2011: Air–sea fluxes from ICOADS: The construction of a new gridded dataset with uncertainty estimates. *Int. J. Climatol.*, **31**, 987–1001, https://doi.org/10.1002/joc.2059.

Bryden, H. L., 1993: Ocean heat transport across 24°N latitude. *Interactions Between Global Climate Subsystems: The Legacy of Hann, Geophys. Monogr.* Vol. 75, Amer. Geophys. Union, 65–75.

——, H. R. Longworth, and S. A. Cunningham, 2005: Slowing of the Atlantic meridional overturning circulation at 25°N. *Nature*, **438**, 655–657, https://doi.org/10.1038/nature04385.

Chafik, L., S. Hakkinen, M. H. England, J. A. Carton, S. Nigam, A. Ruiz-Barradas, A. Hannachi, and L. Miller, 2016: Global linkages originating from decadal oceanic variability in the subpolar North Atlantic. *Geophys. Res. Lett.*, **43**, 10 909–10 919, https://doi.org/10.1002/2016GL071134.

Cunningham, S. A., and Coauthors, 2007: Temporal variability of the Atlantic meridional overturning circulation at 26.5°N. *Science*, **317**, 935–938, https://doi.org/10.1126/science.1141304.

Drijfhout, S., G. J. van Oldenborgh, and A. Cimatoribus, 2012: Is a decline of AMOC causing the warming hole above the North Atlantic in observed and modeled warming patterns. *J. Climate*, **25**, 8373–8379, https://doi.org/10.1175/JCLI-D-12-00490.1.

Duchez, A., and Coauthors, 2016: Drivers of exceptionally cold North Atlantic Ocean temperatures and their link to the 2015 European heat wave. *Environ. Res. Lett.*, **11**, 074004, https://doi.org/10.1088/1748-9326/11/7/074004.

Good, S. A., M. J. Martin, and N. A. Rayner, 2013: EN4: Quality controlled ocean temperature and salinity profiles and monthly objective analyses with uncertainty estimates. *J. Geophys. Res. Oceans*, **118**, 6704–6716, https://doi.org/10.1002/2013JC009067.

Grist, J. P., S. A. Josey, Z. L. Jacobs, R. Marsh, B. Sinha, and E. Van Sebille, 2016: Extreme air–sea interaction over the North Atlantic subpolar gyre during the winter of 2013-2014 and its sub-surface legacy. *Climate Dyn.*, **46**, 4027–4045, https://doi.org/10.1007/s00382-015-2819-3.

Haarsma, R. J., F. M. Selten, and S. S. Drijfhout, 2015: Decelerating Atlantic meridional overturning circulation main cause of future west European summer atmospheric circulation changes. *Environ. Res. Lett.*, **10**, 094007, https://doi.org/10.1088/1748-9326/10/9/094007.

Hansen, B., S. Østerhus, W. R. Turrell, S. Jónsson, H. Valdimarsson, H. Hátún, and S. M. Olsen, 2008: The inflow of Atlantic water, heat, and salt to the Nordic seas across the Greenland–Scotland Ridge. *Arctic–Subarctic Ocean Fluxes*, R. R. Dickson, J. Meincke, and P. Rhines, Eds., Springer, 15–43, https://doi.org/10.1007/978-1-4020-6774-7_2.

——, K. Larsen, H. Hátún, and S. Østerhus, 2016: A stable Faroe Bank Channel overflow 1995–2015. *Ocean Sci.*, **12**, 1205–1220, https://doi.org/10.5194/os-12-1205-2016.

Jochumsen, K., M. Moritz, N. Nunes, D. Quadfasel, K. M. H. Larsen, B. Hansen, H. Valdimarsson, and S. Jonsson, 2017: Revised transport estimates of the Denmark Strait Overflow. *J. Geophys. Res. Oceans*, **122**, 3434–3450, https://doi.org/10.1002/2017JC012803.

Johns, W. E., and Coauthors, 2011: Continuous, array-based estimates of Atlantic Ocean heat transport at 26.5°N. *J. Climate*, **24**, 2429–2449, https://doi.org/10.1175/2010JCLI3997.1.

Josey, S. A., J. J.-M. Hirschi, B. Sinha, A. Duchez, J. P. Grist, and R. Marsh, 2018: The recent Atlantic cold anomaly: Causes, consequences, and related phenomena. *Annu. Rev. Mar. Sci.*, **10**, 475–501, https://doi.org/10.1146/annurev-marine-121916-063102.

Kanzow, T., and Coauthors, 2010: Seasonal variability of the Atlantic meridional overturning circulation at 26.5°N. *J. Climate*, **23**, 5678–5698, https://doi.org/10.1175/2010JCLI3389.1.

Liu, C., and Coauthors, 2017: Evaluation of satellite and reanalysis-based global net surface energy flux and uncertainty estimates. *J. Geophys. Res. Atmos.*, **122**, 6250–6272, https://doi.org/10.1002/2017JD026616.

Lozier, S., and Coauthors, 2019: A sea change in our view of overturning in the subpolar North Atlantic. *Science*, **363**, 516–521, https://doi.org/10.1126/science.aau6592.

McCarthy, G., and Coauthors, 2012: Observed interannual variability of the Atlantic meridional overturning circulation at 26.5°N. *Geophys. Res. Lett.*, **39**, L19609, https://doi.org/10.1029/2012GL052933.

McDonagh, E. L., and Coauthors, 2015: Continuous estimate of Atlantic oceanic freshwater flux at 26.5°N. *J. Climate*, **28**, 8888–8906, https://doi.org/10.1175/JCLI-D-14-00519.1.

Østerhus, S., W. R. Turrell, S. Jónsson, and B. Hansen, 2005: Measured volume, heat, and salt fluxes from the Atlantic to

the Arctic Mediterranean. *Geophys. Res. Lett.*, **32**, L07603, https://doi.org/10.1029/2004GL022188.

Rahmstorf, S., J. E. Box, G. Feulner, M. E. Mann, A. Robinson, S. Rutherford, and E. J. Schaffernicht, 2015: Exceptional twentieth-century slowdown in Atlantic Ocean overturning circulation. *Nat. Climate Change*, **5**, 475–480, https://doi.org/10.1038/nclimate2554.

Rossby, T., C. N. Flagg, K. Donohue, A. Sanchez-Franks, and J. Lillibridge, 2014: On the long-term stability of Gulf Stream transport based on 20 years of direct measurements. *Geophys. Res. Lett.*, **41**, 114–120, https://doi.org/10.1002/2013GL058636.

Schmitz, W. J., Jr., and M. S. McCartney, 1993: On the North Atlantic circulation. *Rev. Geophys.*, **31**, 29–49, https://doi.org/10.1029/92RG02583.

Sévellec, F., A. V. Federov, and W. Liu, 2017: Arctic sea ice decline weakens the Atlantic meridional overturning circulation. *Nat. Climate Change*, **7**, 604–610, https://doi.org/10.1038/nclimate3353.

Smeed, D. A., and Coauthors, 2018: The North Atlantic Ocean is in a state of reduced overturning. *Geophys. Res. Lett.*, **45**, 1527–1533, https://doi.org/10.1002/2017GL076350.

Trenberth, K. E., and J. T. Fasullo, 2017: Atlantic meridional heat transports computed from balancing Earth's energy locally. *Geophys. Res. Lett.*, **44**, 1919–1927, https://doi.org/10.1002/2016GL072475.

Zhang, R., 2008: Coherent surface-subsurface fingerprint of the Atlantic meridional overturning circulation. *Geophys. Res. Lett.*, **35**, L20705, https://doi.org/10.1029/2008GL035463.